Available online at www.sciencedirect.com
SCIENCE DIRECT®
Polymer 44 (2003) 7121–7129
polymer
www.elsevier.com/locate/polymer

Preparation and characterization of composite resin by vinyl chloride grafted onto poly(BA-EHA)/poly(MMA-St)

Mingwang Pan, Liucheng Zhang*, Linzhan Wan, Ruiqiang Guo

Institute of Polymer Science and Engineering, School of Chemical Engineering, Hebei University of Technology, Tianjin 300130, People's Republic of China

Received 7 May 2003; received in revised form 12 August 2003; accepted 12 August 2003

Abstract

Crosslinked poly(butyl acrylate-*co*-2-ethylhexyl acrylate)/poly(methyl methacrylate-co-styrene) (ACR I) latex was synthesized by multi-stage emulsion polymerization. A series of grafting vinyl chloride (VC) composite latices were prepared by emulsion copolymerization in the presence of core-shell ACR I latex. The effects of ACR I amount and its core/shell ratio on particle diameters of the composite latices and mechanical properties of the prepared materials were investigated. The grafting efficiency (GE) of VC grafted onto ACR I increases with an increasing ACR I content. Transmission electron microscope (TEM) study indicates that ACR I latex particles have a regular core-shell structure obviously. However, when styrene content in the shell of ACR I is more than 70 percent of the shell by weight, ACR I latex particles have an irregular core-shell morphology like sandwich. The composite latex particles synthesized by core-shell ACR I latex grafting VC have a clear three-layered core-shell structure. Dynamic mechanical analysis (DMA) study reveals that the compatibility between ACR I and PVC is well improved. With increasing ACR I content, the loss peak in low temperature range for every composite sample becomes stronger and stronger and gradually shifts to a higher temperature. Scanning electron microscope (SEM) graphs showed that the fractured surface of the composite sample exhibited better toughness of the material. TEM graphs showed that ACR I was uniformly dispersed in the PVC matrix.

Keywords: Poly(vinyl chloride); Core-shell polymers; Emulsion polymerization

1. Introduction

There are some deficiencies for polyvinyl chloride resin by emulsion polymerization technique such as low notched-impact strength, bad thermal aging property and weatherability and the like. For a long time, people have been devoting themselves to modification for PVC resin [1–7]. A conventional blend modification is generally utilized by another crosslinked rubbery polymer added into PVC resin. But there is comparatively poor compatibility between PVC and rubbery polymer. Then the modified effect for PVC resin is little significant.

Moreover, an important part of PVC production is processed with plasticizers to give flexible products. The adding amount of plasticizers determines ductility, flexibility, and freezing resistance of the products. However, soften point temperature and modulus of the product would decrease greatly, and a migration of the plasticizers onto the surface is another undesirable property of this kind of products. The plasticizer is gradually lost from the surface due to evaporating or dissolution with liquids that are often in contact with the product. Consequently, the PVC product starts to be more rigid, shrinks, and cracks. In addition, the leached plasticizer pollutes the environment around the products. And in the heating process, the PVC resin with adding plasticizer will be oxidized to result in decomposition.

Based on the above-mentioned facts, the aim of this research is to prepare a new kind of emulsion PVC resin with an improved impact resistance. Compared with other modifiers useful in impact modification of PVC, core-shell polyacrylate has more excellent elasticity and weatherability. Hence, core-shell polyacrylate used as the impact modifier of PVC is adopted in this paper. A series of composite emulsion resin were synthesized by grafting of vinyl chloride (VC) onto the core-shell poly(BA-EHA)/poly(MMA-St) (abbreviated to ACR I) latex, the core of which was composed of butyl acrylate and 2-ethylhexyl acrylate

* Corresponding author. Tel.: +86-22-26582054; fax: +86-22-26371547.
E-mail address: panmingwang@eyou.com (L. Zhang).

0032-3861/$ - see front matter © 2003 Elsevier Ltd. All rights reserved.
doi:10.1016/j.polymer.2003.08.022

copolymer and the shell layer of which was synthesized using methyl methacrylate and styrene [8–11]. We try to find a desirable preparing procedure to solve the questions about aggregation or heterogenetic dispersion of rubber particles in PVC blends. Namely, the toughening efficiency of rubbery polymer gets an improvement by the preparing procedure. Meantime, the good mechanical properties of PVC resin are preserved to a large extent.

2. Experimental

2.1. Chemicals

The monomers, *n*-butyl acrylate(BA), 2-ethylhexyl acrylate(EHA), styrene(St), methyl mechacrylate(MMA), 1,4-butylene glycol diacrylate(BDDA), industrial product, all monomers were supplied by the Beijing dong fang chemical plant, freshly distilled under reduced pressure and stored at −10 °C prior to use. Sodium dodecylsulfate (SDS), chemically pure, used as an emulsifier. Potassium persulfate ($K_2S_2O_8$), chemically pure, recrystallized, used as an initiator. Sodium tetraborate ($Na_2B_4O_7$), chemically pure, is the pH modifying agent. Vinyl chloride (VC), above 99.99 wt% purity, supplied by the Tianjin chemical plant. Calcium stearate, stearyl alcohol, chemically pure, and organotin stabilizer, commercial grade, supplied by the Tianjin chemical company.

2.2. Synthesis of core-shell poly(BA-EHA)/poly(MMA-St) (ACR I) latex

A 500 mL of four-necked glass flask was charged with 200 g of distilled water, 0.50 g of SDS, 7.1 g of BA, 3.9 g of EHA, 0.16 g of BDDA and 0.12 g of $K_2S_2O_8$ with agitation, while nitrogen was adjusted to sweep the atmosphere over the reaction mixture. After 30 min, 0.75 g of $Na_2B_4O_7$ in 30 g of water were added to adjust the pH of the reaction mixture between 8 and 9. Meantime, the contents of the reactor were heated to 80 °C. In the first or seed stage, the polymerization was held at 80 °C for 1 h, then chased with 0.50 g of SDS in 25 g of distilled water over 10 min.

In the second or 'core' stage, 0.25 g of $K_2S_2O_8$ in 25 g of distilled water over 10 min were firstly added into the reactor. 28.6 g of BA, 15.4 g of EHA, 0.66 g of BDDA are premixed with agitation. Then above premixed solution was begun to dropwise over a 1.5-hour period. The reaction was maintained for another 2 h.

In the third or 'shell' stage, a chase of 0.20 g of $K_2S_2O_8$ in 25 g of distilled water were firstly added into the reactor over 10 min. The mixture of 26.0 g of MMA, 11.5 g of St, 0.37 g of BDDA was gradually added in over a 60-minute period. The reaction was maintained for another 2 h. Then the core-shell poly(BA-EHA)/poly(MMA-St) latex was obtained.

2.3. Preparation of composite resin in emulsion

A 2 liter-stainless steel autoclave was charged with 900 mL of deionized water, 2.0 g of SDS, 0.70 g of $K_2S_2O_8$ and a determined amount of poly(BA-EHA)/poly(MMA-St) latex with agitation. Five weight percent of the sodium hydroxide solution was utilized to adjust the pH of the reactive mixture between 9.5 and 10.5. After closing and evacuating the reaction vessel, 400 g of the VC monomer was introduced into the reactor. The contents of the reactor were heated to 50 °C. The copolymerization was maintained at 50 ± 0.3 °C until the pressure decreased to 0.35 MPa. The seeded emulsion copolymerization was short-terminated. After cooling, the unreacted monomer was removed. The composite resin was isolated from the emulsion by freezing coagulation, followed by filtration, rinsed by deionized water, and dried under reduced pressure at 50 °C.

2.4. Particle diameter measurement of ACR I and composite latices

The particle diameters and their distribution of ACR I and the composite latices were measured with the aid of a Coulter Model N4MD submicron particle analyzer (Coulter Electronics Inc.) and a H-800 transmission electron microscope.

2.5. Determination of grafting efficiency (GE)

ACR I-grafted vinyl chloride resin is substantially a mixture which is composed of the homopolymer of PVC, crosslinked ACR I and the ACR I-grafted VC copolymer. So, the determination of the GE requires some means of separating the PVC homopolymer from ACR I -grafted VC composite resin [12–15]. This is achieved by extraction with tetrahydrofuran, which removes the PVC, which is not grafted onto ACR I, but the crosslinked ACR I and its grafted vinyl chloride copolymer remain. In the experiment, a weighed amount of the composite resin was sealed in a special paper bag, placed in a Soxhlet thimble, and extracted with tetrahydrofuran for 24 h. The undissolved polymer was dried, weighed, and again extracted with tetrahydrofuran for additional hours. This process was repeated until no further weight loss was observed. The chlorinity of the undissolved polymer was determined by elementary analysis in order to calculate the grafted PVC amount. The GE was determined by dividing the amount of PVC, which was grafted onto ACR I by the total amount of PVC present before extraction. It can be calculated by the following equation:

$$\mathrm{GE} = \frac{{}_{a}\dfrac{M_1}{M_2}{}_{X}}{{}_{b+a}\left(\dfrac{M_1}{M_2}{}_{X-1}\right)}$$

where a is the mass of the undissolved polymer; b, the original mass of the sample before extraction; M_1, the

molecular weight of vinyl chloride; M_2, the chlorine atomic weight, X, the chlorinity of the undissolved polymer.

2.6. Preparation of composite sample

The synthesized composite resin was mixed with a determined quantity of additives. The processing recipe was 100 parts of composite resin, 2.5 parts of organotin, 0.8 part of calcium stearate, and 0.8 part of stearyl alcohol. All components were first premixed in a high-speed mixer at room temperature and then processed on a laboratory two-roll mill between 170 and 175 °C for 7 min. Two- or four-millimeter-thick plates were pressed at the temperature of 178–182 °C. The plates were cooled under a cooling press. Dumbbell-shaped samples for the tensile test were cut from the plates. The size of the samples for the notch impact test was $55 \times 6 \times 4$ mm^3, the notch depth was equal to 1/3 of the thickness of the sample.

2.7. Determination of mechanical properties

Tensile strength testing was performed using an RGT-10A electronic tensile tester with computer controlling system. The testing portion of the dumbbell specimen was 25 mm long with a cross-section of 2×6 mm^2. Tests were conducted at an extension rate of 20.0 mm min^{-1} at 23 °C and 50% relative humidity. The notched impact strength was carried out on an XCJ-40 Charpy impact tester.

Dynamic mechanical measurements were carried out using a Netzsch DMA242(Germany)-type dynamic mechanical analyzer. The measuring frequency was 1 Hz; the heating rate, 3 K/min; and the temperature range, from −110 to +130 °C.

2.8. Electron microscopy

The morphology of the composite samples was characterized by an S-250 scanning electron microscope (SEM). The fractured surface of the notched impact bar was coated with a thin layer of gold under a vacuum. The morphology of ACR I and the composite latex particles and the separation of rubbery copolymer in the samples were observed through a Hitachi EM-H-800 transmission electron microscope (TEM) in conjunction with the RuO_4-staining method. The P(BA-EHA) and polystyrene phases in the samples can be stained.

3. Results and discussion

3.1. Latex particle diameters and their distribution

The particle diameter distributions of ACR I and composite latices are shown in Fig. 1.

As seen from Fig. 1, the particle diameter distribution of the composite latex is similar to that of the ACR I latex and shows a relatively narrow single peak. However, the mean particle diameter (MPD = 196 nm) of the composite latex has increased much more than that of the seeded ACR I (MPD = 107 nm).

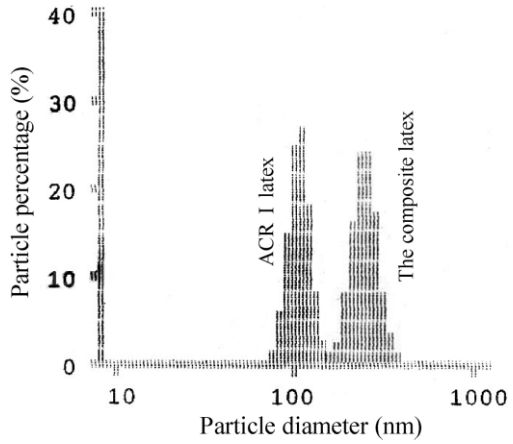

Fig. 1. Particle diameter distribution of ACR I and the composite latex.

When the amount of the ACR I latex in copolymerization system was varied, keeping other conditions unchangeable, the MPD of the synthetic composite latex as a function of the ACR I content was shown in Fig. 2.

Fig. 2 indicates that the MPD of the composite latex gradually decreases with an increasing ACR I content. Because of increasing the amount of ACR I, the number of latex seeds, used as the VC grafted copolymerization, obviously increase for the same VC feeding amount. So the MPD of the formed composite latex decreases. However, each MPD of all the composite latices is much larger than the MPD (107 nm) of pure ACR I latex, respectively. Moreover, the MPD of the prepared PVC latex was only about 78 nm without the ACR I latex as the seed. All these above-mentioned would suggest that PVC macromolecular chains grow on the surfaces of ACR I particles and the core-shell composite particles were formed, as observed in Fig. 3(c).

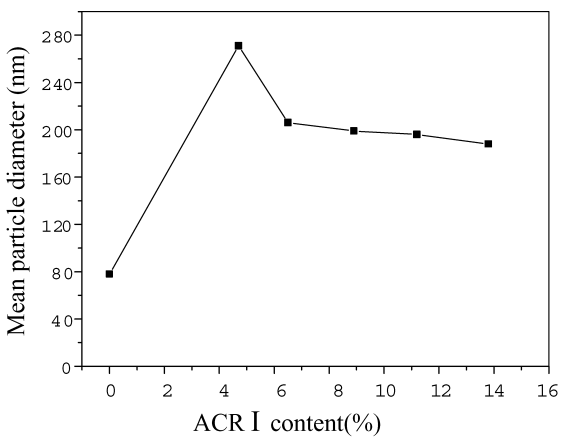

Fig. 2. Influence of ACR I amount on mean particle diameter of composite latices.

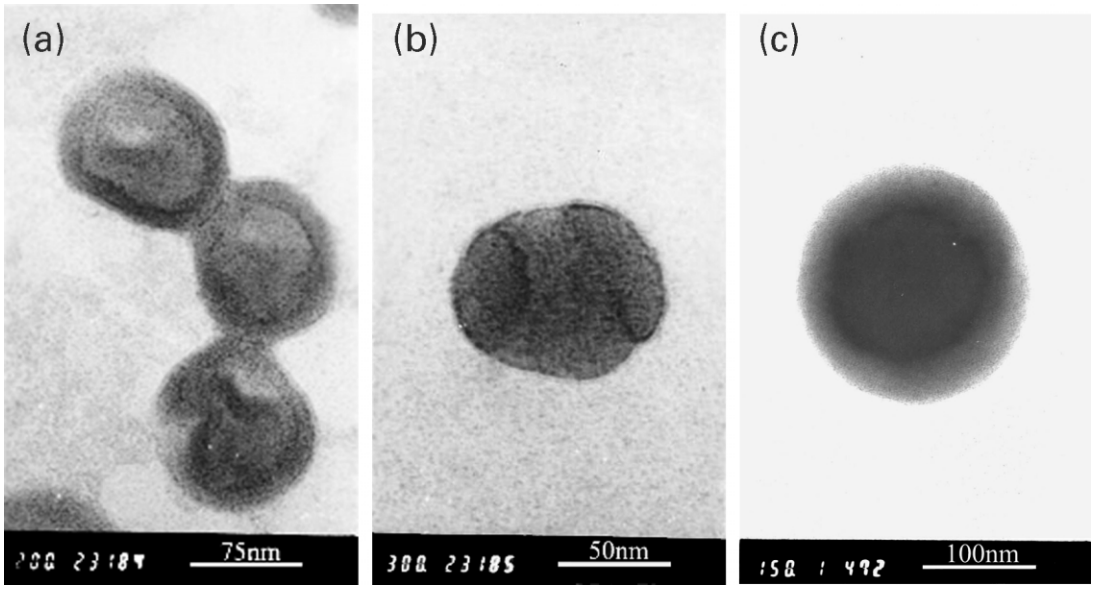

Fig. 3. TEM photographs of ACR I with core-shell ratio of 60/40 and composite latex particles (a) ACR I (BA%:65%, St%:40%); (b) ACR I (BA%:65%, St%:75%); (c) composite latex (ACR I content: 6.5 wt% solid).

3.2. Morphology of ACR I and composite latex particles

When the proportion between MMA and St in the shell of ACR I was varied in an otherwise fixed condition, different morphology of the ACR I latex particles was observed through the TEM study. As shown in Fig. 3(a), the morphology of the ACR I latex particles has, obviously, a regular core-shell structure. The light-colored portion in the core of the ACR I latex particle is the P(BA-EHA) rubbery copolymer. The deeper-black portion in the shell of the ACR I latex particle is the poly(MMA-St) copolymer. The reason is that polystyrene phase in the shell is more easily stained by RuO_4 than the P(BA-EHA).

However, experimental study discovered that when polystyrene content in the shell of ACR I was more than 70% of the shell by weight, the particle of ACR I latex has an irregular core-shell structure like sandwich, as shown in Fig. 3(b). The experimental result confirms that styrene molecules or polystyrene chain segments would easily migrate into the core of ACR I to result in latex particles with an abnormal core-shell structure formed.

The morphological structure of the composite latex particle observed by the TEM study is shown in Fig. 3(c). As seen from Fig. 3(c), the morphology of the composite latex particle obtained by ACR I-grafted VC has a clear core-shell structure with three layers. The core is the P(BA-EHA) elastomer. Certainly, in the process of preparing composite latex, the cross-linked ACR I latex particles could be swollen by a large number of VC monomers due to their diffusion. These VC monomers were initiated to form many PVC micro-particles existing in the ACR I. This made apparent rubbery volumes increased. The middle-thin layer, whose color is the deepest in the particle, is the poly(MMA-St) phase. As above-mentioned, RuO_4-staining polystyrene phase is easier than the P(BA-EHA) and PMMA, while staining PVC is the most difficult. Then the light-colored portion in the shell of the composite particle is mainly PVC. So, it can be just seen from Fig. 3(c) that the ACR I latex particle was encapsulated by PVC.

3.3. Effect of ACR I content on grafting efficiency

From Fig. 4, it can be seen that the GE increases as the ACR I content is increased. This was expected. Because the emulsion copolymerization system is heterogeneous, for feeding the same quantity of VC monomer, by increasing the ACR I latex amount, the probability of contact between the VC monomer and the backbone ACR I increases. Hence, the probability or the amount of VC grafted onto ACR I increases. So, the GE is enhanced.

Generally, activation of alpha-carbon in the ACR I macromolecules is assumed based on the activation by the

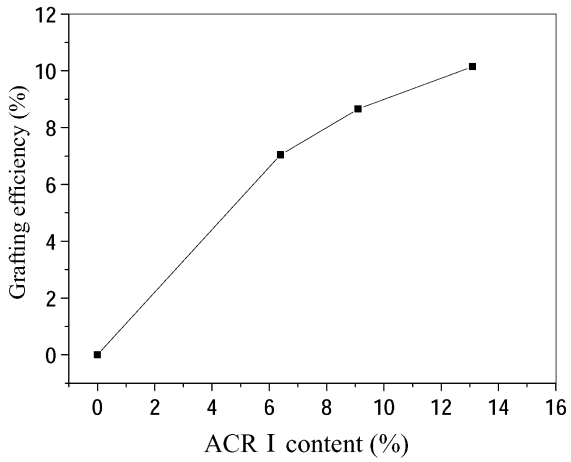

Fig. 4. Influence of ACR I content on grafting efficiency.

carbonyl group and consequent lowering of strength of the C–H bond on the alpha-carbon in comparison with other C–H bonds [14]. Moreover, this kind of macro-radical is stabilized by the effect of the ester and benzene groups. Especially for VC monomer, its chain transfer constant is the greater than other common monomers and greatly increases with polymerization temperature. In the process of preparing composite latex, the cross-linked ACR I latex particles were swollen by VC monomers. So, the VC monomers, including PVC macro-radicals, can enter a reaction with the activated carbon (or radical) in the ACR I easily.

A Fourier transform infrared spectrometer (FTIR) was used to study the structural changes in the ACR I after grafting PVC in order to determine how the chain transfer grafting took place [15]. The grafting mechanism was revealed through relative intensity changes between the two absorption peaks of the CH_2 group at 1427 cm^{-1} and the CH group at 1255 cm^{-1}. The FTIR study implies that chain transfer occurs via removing hydrogen atom from ACR I macromolecules. See also the Ref. [16] for the more detailed results.

3.4. Dynamic mechanical analysis (DMA) and mechanical properties

3.4.1. Dynamic mechanical analysis of composite samples

Fig. 5 shows dynamic mechanical spectra of the composite resin with different ACR I contents, ACR I and pure PVC.

As seen from Fig. 5, there are two distinct spectral peaks for every curve. There is a wide β-secondary transition peak near −57 °C at 1 Hz for the PVC sample. For the composite resin, the intensity of the mechanical loss peak (tan δ) in the temperature range of −50 to +10 °C is markedly dependent on the increment of the ACR I content. And the maximum values of the loss peak positions gradually shift to higher temperature with an increasing ACR I content. The influence of ACR I content on glass transition temperatures (Tg) of the samples is shown in Table 1.

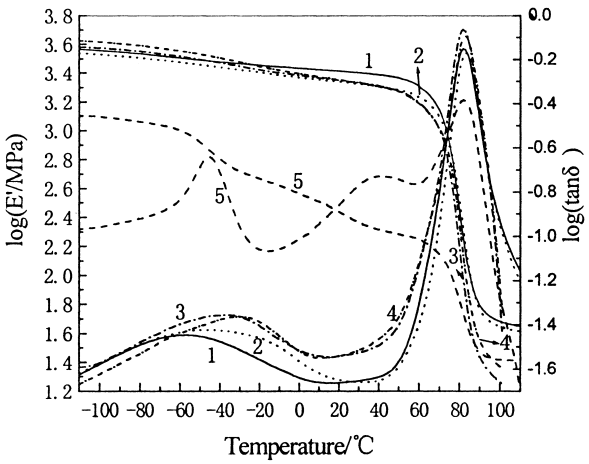

Fig. 5. DMA spectra of composite samples ACR I content: (1) 0.0 wt% (pure PVC); (2) 6.5 wt%; (3) 8.9 wt%; (4) 13.8 wt%; (5) 100 wt% (pure ACR I).

The low-temperature transition of the composite resin is mainly attributed to the glass transition of the P(BA-EHA) rubbery copolymer and the β-secondary transition of PVC and PMMA. The effect of the β-secondary transition of PVC on the transition temperature in low-temperature range (T_{g1}) of the composite sample is almost neglectful with increment of the ACR I content. The T_{g1} of ACR I is −45.4 °C. The experimental datum was higher than the T_g of pure PBA (T_g, −55 °C) or PEHA (T_g, −85 °C) in the literature. This discrepancy may be caused by the higher degree of crosslinking in the core of ACR I, and the T_{g1} closely depends on the proportion between PBA and PEHA in the core of ACR I.

The dynamic mechanical spectra demonstrate that the maximum position of the loss peak in low-temperature range (T_{g1}) for the composite resin is markedly different from that of ACR I and pure PVC. As shown in Table 1, the difference of the T_{g1} might be related to the diffusion of VC monomer into the cross-linked ACR I to form the grafting transition region with interpenetrating polymer networks. For the same adding amount of the VC monomer, the more the amount of the ACR I feed is, the greater the number of the formed composite particles is. Then, the enhanced grafting efficiency gives rise to an increased T_{g1} of the composite resin in the low-temperature transition region, namely, the distance ($T_{g2}-T_{g1}$) between the two (tan δ) loss peaks in low- and high-temperature range becomes shorter. The ACR I-grafted VC copolymer formed in the composite resin is helpful to increasing the compatibility between the ACR I and PVC phases. DMA results imply that the compatibility between the P(BA-EHA) and PVC should have been well improved. Moreover, the storage modulus of the composite samples decreases less with temperature in contrast with that of PVC, as shown in Fig. 5.

3.4.2. Effect of ACR I content on impact strength of the material

Fig. 6 presents the impact strength results of the materials with varying ACR I content.

As shown in Fig. 6, the notched impact strength of the

Table 1
Influence of ACR I content on glass transition temperatures of the samples

Sample no.	T_{g1} (°C)	T_{g2} (°C)	$T_{g2}-T_{g1}$ (°C)	ACR I content (wt%)
1	−56.9 (β peak)	82.3	139.2	0.0
2	−46.2	83.3	129.5	6.5
3	−37.2	82.0	119.2	8.9
4	−29.4	83.0	112.4	13.8
5	−45.4	82.2	127.6	100.0

T_{g1} and T_{g2} mean glass transition temperatures in low and high temperature range, respectively.

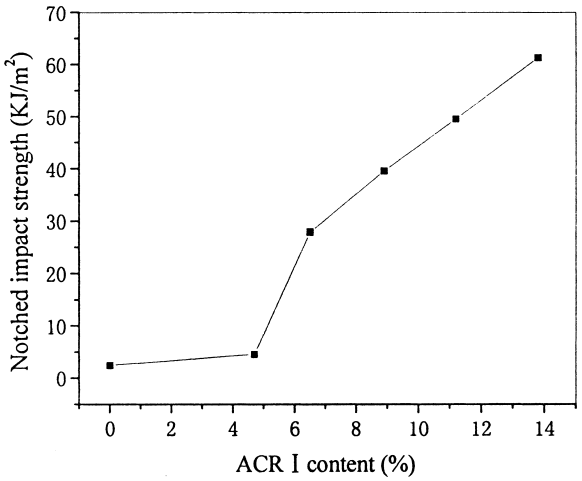

Fig. 6. Influence of ACR I content on notched impact strength of materials.

materials pronouncedly increases with an increasing ACR I content at room temperature. Wu.S. [17–19], Groeninckx et al. [20,21] claimed that substantial enhancement of the toughness of brittle or notch-sensitive polymers can be achieved by dispersing rubber particles in the polymer matrix. In pseuoductile thermoplastic matrices, which deform preferentially by shear yielding, the major toughening mechanisms are thought to be cavitation of the rubbery particles and shear yielding of the matrix. The transition from brittle to ductile behavior in rubber-modified pseuoductile thermoplastics occurs at a critical value of the interparticles distance (IPD), which is given by the following:

$$\mathrm{IPD} = d_0\{(\pi/6\phi_r)^{1/3} - 1\},$$

where d_0 is the particle diameter of the rubber particle, and φ_r, the rubber volume fraction.

In this paper, the MPD of the synthesized ACR I particles is about 107 nm, whereas the average size of the rubbery cores is about 90 nm. When the ACR I content is less than 6 wt% of the material, the IPD of rubbery particles is probably greater than the critical IPD. Then, shear yielding of the matrix occurs not easily, and the toughness of the material is not improved markedly. On the contrary, then the result is just the contrary.

Here, core/shell ratio of ACR I is 60/40. Toughening effect of ACR I is chiefly dependent on its elastic core. Its shell layer can improve the compatibility between the core of ACR I and PVC. The P(BA-EHA) elastomer is a pliable component in the material. When the material is subjected to impact force with high speed, the 'craze-shear band' theory claimed that the rubbery particles become centers of stress concentration and initiate crazes or shear bands in the matrix. While crazes or shear bands occur and grow, a large amount of energy is absorbed in this region. On the other hand, these pliant particles and the interaction between crazes and shear bands can confine the development of crazes and prevent crazes becoming cracks from the breaking of materials. When the ACR I content is less (such as 4 wt%), the less number of rubbery particles can only initiate less crazes or shear bands. Then, the impact strength of the material is not enhanced significantly. Therefore, the greater ACR I content is, the more crazes and shear bands the ACR I particles will initiate. Thus, more energy will be absorbed and the impact strength of the materials will be greatly enhanced.

3.4.3. Effect of core/shell ratio of ACR I on mechanical strength of the material

Varying core/shell ratio of ACR I in an otherwise fixed condition, the composite resin with different core/shell ratios of ACR I was prepared under the same ACR I content. The mechanical strength of the prepared materials is shown in Fig. 7.

As shown in Fig. 7, the notched impact strength of the materials obviously enhances with an increasing the core/shell ratio of ACR I. Because the toughening effect of ACR I is chiefly attributed to the apparent volume of its core layer or rubbery phase, increasing the core/shell ratio of ACR I means increasing the effective volume for the same adding amount of ACR I toughening modifier. For the sample with the core/shell ratio of ACR I being 90/10, its notched impact strength was not improved markedly. Its reason is related to ACR I itself not forming a regular core-shell structure.

The tensile strength of the prepared materials somewhat decreases with an increasing core/shell ratio of ACR I, as shown in Fig. 7.

3.4.4. Influence of ACR I content on tensile strength and elongation at break of the materials

The influence of the ACR I content on the tensile strength and the elongation at break of the materials is shown in Fig. 8.

As is seen from Fig. 8, the tensile strength of the materials gradually decreases with an increasing ACR I content, but the elongation at break of the materials markedly increases. While the notched impact strength of

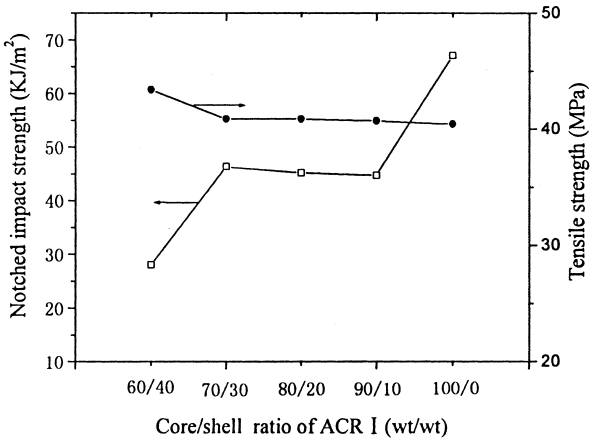

Fig. 7. Influence of core/shell ratio of ACR I on tensile strength and impact strength of materials (ACR I content: 6.5 wt%).

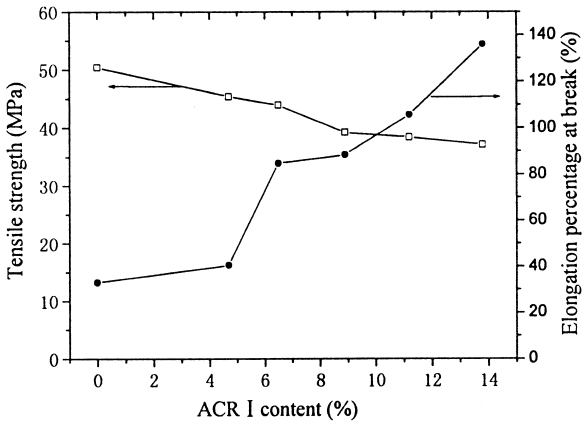

Fig. 8. Influence of ACR I content on tensile strength and elongation at break of materials.

the material is enhanced to near 11 times as large as that of pure PVC, its tensile strength is approximately 87% of the tensile strength of pure PVC, and its elongation at break is about two and half past times that of PVC. By increasing the ACR I content, the elongation at break of the composite samples is continually improved.

3.5. SEM and TEM analyses

SEM graphs of the impact breaking surfaces of pure PVC and the composite samples with different ACR I contents are shown in Fig. 9(a)–(d), respectively.

As seen from Fig. 9(b)–(d), the fractured surface of the notched impact sample with 4.7 wt% ACR I is some rough and looks like a crisscross shape (Fig. 9(b)). It appears that the material begins a transition from a fragile to toughness. The fractured surface of the composite sample with 6.5 wt% ACR I has a morphology like interpenetrating networks or a ripple shape (Fig. 9(c)). It shows that an extensive plastic-shearing deformation of the PVC matrix has happened, and the better toughness of the material is exhibited. There are many micro-holes with different sizes and polymer strings on the breaking surface for the composite sample with 8.9 wt% ACR I, as shown in Fig. 9(d). An extensive plastic deformation of the PVC matrix is evidenced by the appearance of numerous strings, cavitation or the voids formed by debonding of some particles from the PVC matrix [22–24]. Hence, the morphological features of the fractured surfaces for the composite samples correspond to the impact-resistant toughness of the materials. In contrast to the composite samples, the fractured surface of pure PVC shown in Fig. 9(a) is smooth, clear and sharp. It exhibits a distinct brittle breakage of pure PVC. So, the PVC sample shows a poor notched impact property.

The TEM graphs of the composite samples corresponding to (c) and (d) are shown in Fig. 9(e) and (f), respectively. The morphology of the composite samples has a two-phase structure with micro-phase separation. The morphological structure is consistent with the result of the DMA for them. And the greater the ACR I content is, the higher the concentration of the ACR I particles in the composite samples is, more greatly the toughness of the sample is enhanced, as shown in Figs. 6 and 9.

Compared with usual blend modification, the P(BA-EHA) rubbery phase in this system was much uniformly dispersed in the PVC matrix. This good distribution stemmed from ACR I particles well encapsulated by PVC macromolecules to avoid an aggregation of the ACR I particles. The good dispersion of the P(BA-EHA) is very helpful to improving toughening efficiency of the rubbery polymer. The compatibility between ACR I and PVC was improved due to the ACR I-grafted VC copolymer and PMMA. So, the observed interface between the P(BA-EHA) and PVC was indistinct.

4. Conclusions

The MPDs of the composite latices gradually decrease with an increasing amount of ACR I latex. PVC macromolecules have encapsulated ACR I particles to form the composite particles with a three-layered core-shell structure. ACR I latex particles have a regular core-shell structure. While styrene content in the shell of ACR I was more than 70% of the shell by weight, ACR I latex particles with abnormal core-shell morphology like sandwich were observed. The GE increases with an increasing ACR I content.

There are two distinct transition peaks for every composite sample as shown by the dynamic mechanical spectra. Compared with pure PVC, every mechanical loss peak for all the samples is stronger in the low-temperature transition region. Further, the maximum value of the loss peak gradually shifts to a higher temperature with an increasing ACR I content. Then, the distance ($T_{g2}-T_{g1}$) between the two loss-peaks for every composite sample becomes shorter with an increment of ACR I. The compatibility between ACR I and PVC has been well improved.

The notched impact strength and elongation at break of the materials greatly increase with an increasing ACR I content, whereas the tensile strength of the materials decreases a little. The notched impact strength of the prepared materials is obviously enhanced with an increasing core/shell ratio of ACR I. The fractured surface of the notched sample for the composite sample exhibits good toughness. Its morphology is consistent with showing toughness of the materials. The P(BA-EHA) rubbery phase in the materials is uniformly dispersed in the PVC matrix. Here, the developed composite resin is a promising raw material for manufactures of many products. It will be expected to realize industrialization and widely applied in many fields in the near future.

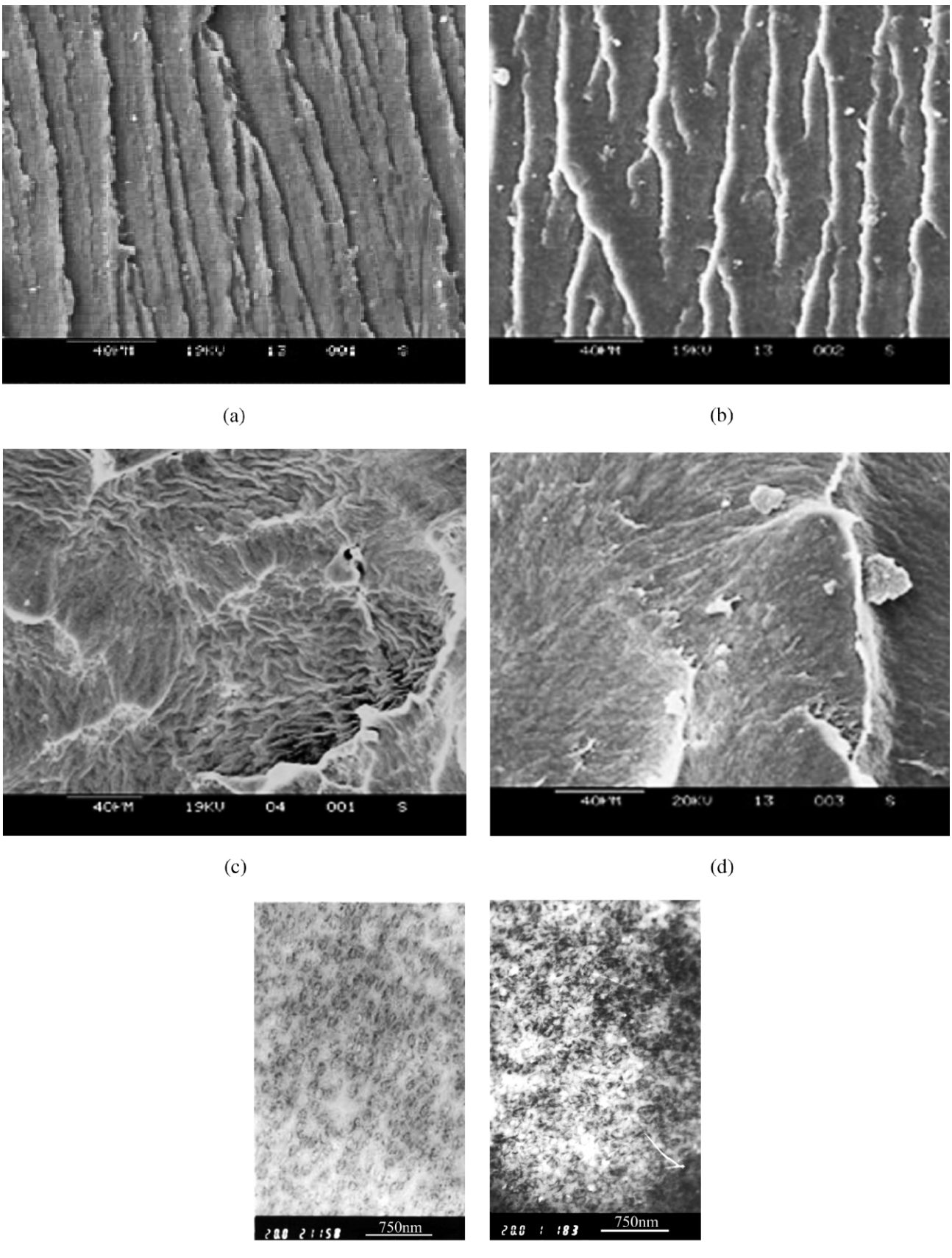

Fig. 9. SEM and TEM photographs of samples. (a) ACR I content: 0 wt% (PVC); (b) ACR I content: 4.7 wt%; (c) ACR I content: 6.5 wt%; (d) ACR I content: 8.9 wt%; (e) ACR I content: 6.5 wt%; (f) ACR I content: 8.9 wt%.

Acknowledgements

This work was supported by the Major Program of Hebei Province in China (No. 01213074D).

References

[1] Rozkuszka KP, Weier JE. US Pat 1997; 5,612,413.
[2] Wills MC, Roebling NJ. US Pat 1994; 5,312,575.
[3] Troy EJ, Rosado A. US Pat 1996; 5,534,594.
[4] Gao JG, Yang LT, Deng KL, Yao ZH. Polymer 1997;38:1139.
[5] Zhang LC, Li XC, Liu TC. J Appl Polym Sci 1991;42:891.
[6] Zhang LC, Tai HW, Liu YD. Polym Advan Tech 1996;7:281.
[7] Zhang LC, Li XC, Liu TC. In: Klempner D, Sperling LH, Utracki LA, editors. Three-stage latex interpenetrating polymer networks. Advances in Chem. Ser. No. 239, Washington, DC: American chemical Society; 1994. Chapter 19.
[8] Oomura T, Hatakeyama H, Suenaga Y. JP Pat 1999;11 228,642 A2.
[9] Fujii N, Shinko T. JP Pat 1999;11 181,033 A2.
[10] Seiki A, Matsumura K. JP Pat 2000; 2000 38,493 A2.
[11] Huo JS. Petrochem Tech 1998;27:253.
[12] Zhang XC, Wang LL, Qian BG. Angew Makromol Chem 1993;209:1.
[13] Macho V, Králik M, Micka M, Komora L, Bakoš D. J Appl Polym Sci 1998;68:649.
[14] Macho V, Králik M, Micka M, Komora L, Srokova I. J Appl Polym Sci 2002;83:2355.
[15] Zhou ZM, Zhu M, Wu XD, Qian DZ. Polymer 1994;35:2888.
[16] Pan MW. Dissertation for the Doctoral Degree, Hebei University of Technology, Tianjin, People's Republic of China; 2003.
[17] Wu SH. Polymer 1985;26:1855.
[18] Wu S. J Appl Polym Sci 1988;35:549–61.
[19] Wu S. Polym Int 1992;29:229.
[20] Dompas D, Groeninckx G. Polymer 1994;35:4743.
[21] Dompas D, Groeninckx G, Isogawa M, Hasegawa T, Kadokura M. Polymer 1994;35:4750. 4760.
[22] Hourston DJ, Lane S, Zhang HX. Polymer 1991;32(12):2215–20.
[23] Crawford E, Lesser AJ. Polymer 2000;41:5865–70.
[24] Yanagase A, Ito M, Yamamoto N, Ishikawa M. J Appl Polym Sci 1996;60:87.